DOI: 10.1534/genetics.108.087924

Quantitative Trait Loci Mapping of Genome Regions Controlling Permethrin Resistance in the Mosquito *Aedes aegypti*

Karla Saavedra-Rodriguez,*,† Clare Strode,‡ Adriana Flores Suarez,† Ildefonso Fernandez Salas,† Hilary Ranson,‡ Janet Hemingway‡ and William C. Black IV*,[1]

**Department of Microbiology, Colorado State University, Fort Collins, Colorado 80523-1685,* †*Laboratorio de Entomologia Medica, Facultad de Ciencias Biologicas, Universidad Autonoma de Nuevo Leon, 66451 México, and* ‡*Vector Group, Liverpool School of Tropical Medicine, Pembroke Place, Liverpool L3 5QA, United Kingdom*

Manuscript received February 11, 2008
Accepted for publication July 7, 2008

ABSTRACT

The mosquito *Aedes aegypti* is the principal vector of dengue and yellow fever flaviviruses. Permethrin is an insecticide used to suppress *Ae. aegypti* adult populations but metabolic and target site resistance to pyrethroids has evolved in many locations worldwide. Quantitative trait loci (QTL) controlling permethrin survival in *Ae. aegypti* were mapped in an F_3 advanced intercross line. Parents came from a collection of mosquitoes from Isla Mujeres, México, that had been selected for permethrin resistance for two generations and a reference permethrin-susceptible strain originally from New Orleans. Following a 1-hr permethrin exposure, 439 F_3 adult mosquitoes were phenotyped as knockdown resistant, knocked down/recovered, or dead. For QTL mapping, single nucleotide polymorphisms (SNPs) were identified at 22 loci with potential antixenobiotic activity including genes encoding cytochrome P450s (CYP), esterases (EST), or glutathione transferases (GST) and at 12 previously mapped loci. Seven antixenobiotic genes mapped to chromosome I, six to chromosome II, and nine to chromosome III. Two QTL of major effect were detected on chromosome III. One corresponds with a SNP previously associated with permethrin resistance in the *para* sodium channel gene and the second with the *CCEunk7o* esterase marker. Additional QTL but of relatively minor effect were also found. These included two sex-linked QTL on chromosome I affecting knockdown and recovery and a QTL affecting survival and recovery. On chromosome II, one QTL affecting survival and a second affecting recovery were detected. The patterns confirm that mutations in the *para* gene cause target-site insensitivity and are the major source of permethrin resistance but that other genes dispersed throughout the genome contribute to recovery and survival of mosquitoes following permethrin exposure.

DENGUE and yellow fever are caused by flaviviruses transmitted by mosquitoes. The principal vector of these flaviviruses on a worldwide basis is the mosquito *Aedes aegypti*. Dengue fever has become the most prevalent arboviral disease causing morbidity and mortality in most tropical regions (Gubler 2005) and dengue control campaigns rely on a small group of insecticides to prevent disease outbreaks. The most common insecticides for larval *Ae. aegypti* control are an organophosphate compound called temephos and a carbamate called propoxur. Both of these compounds bind noncompetitively to and inhibit the activity of the enzyme acetylcholine esterase at nerve synapses eventually leading to the buildup of the neurotransmitter acetylcholine and preventing nerve transmission. Adult *Ae. aegypti* control instead relies on pyrethroids and, a synergist, piperonyl butoxide which is a potent cytochrome P450 inhibitor that can act as the principal detoxification pathway for many insecticides. The pyrethroids are axonic poisons that bind to sodium-gated channels in neuronal membranes causing nerve cells to produce repetitive discharges and eventually paralysis. Both acetylcholine esterase inhibitors and axonic poisons are usually used to reduce selection for resistance associated with use of the same class of insecticide on both larvae and adults (Norma Oficial Mexicana 2003).

Nevertheless, as a result of constant insecticide pressure, *Ae. aegypti* populations have inevitably evolved resistance mechanisms that include target-site insensitivity and high levels of metabolic detoxification. In México, *Ae. aegypti* populations from Baja California have elevated metabolic resistance associated with esterases (Flores *et al.* 2005). In the Yucatán Peninsula, target-site resistance occurs as well as metabolic resistance associated with high levels of esterases and oxidases (Flores *et al.* 2006). Cuban and Venezuelan populations of *Ae. aegypti* have been well characterized for target-site insensitivity (Bisset *et al.* 2006) and various forms of metabolic resistance (Rodriguez *et al.* 2001, 2002, 2005).

Until recently, identification of metabolic detoxification mechanisms have relied upon synergist bioassays

[1]*Corresponding author:* Department of Microbiology, Immunology, and Pathology, Colorado State University, Fort Collins, CO 80523-1685. E-mail: wcb4@lamar.colostate.edu

and broad-spectrum biochemical tests (Brogdon and McAllister 1998a). However, in *Ae. aegypti* there are 26 glutathione transferases, 160 cytochrome P450s, 49 carboxy/cholinesterases, and 67 genes encoding proteins with various types of oxidase activities (Strode *et al.* (2008). This high diversity of detoxification enzymes and difficulties associated with enzyme isolation and characterization has prevented an understanding of the involvement of individual genes in the overall detoxification pathway. Targeted microarray chips containing CYP, EST, GST, and various oxidase genes discovered in genome projects have been used to identify specific genes with elevated levels of transcription in resistant strains of the principal malaria vectors, *Anopheles gambiae* (David *et al.* 2005), *An. stephensi* (Vontas *et al.* 2007), and *Ae. aegypti* (Strode *et al.* (2008). These targeted arrays greatly simplified screening for the principal enzymes involved in insecticide detoxification. Limitations associated with the use of targeted microarray chips are that only those genes printed on the chip can be examined and only those genes whose function is related to changes in transcriptional activity can be identified. While proteomic approaches toward identifying resistant genes in *Drosophila melanogaster* have been developed (Pedra *et al.* 2005), similar tools have not been applied in mosquitoes.

Quantitative trait loci (QTL) mapping is a tool that can be used to identify genome regions associated with insecticide resistance. The power of QTL mapping is that it does not require the use of candidate genes and also makes no assumptions about resistance mechanisms. It can instead be used to test whether candidate genes are associated with resistance phenotypes in a controlled, common environment in the laboratory. QTL mapping may also eventually lead to the identification of novel transcription factors and regulatory elements that regulate the CYP, EST, and GSTs that directly metabolize insecticides. QTL mapping was used to identify genome regions conferring DDT and pyrethroid resistance in *An. gambiae* (Ranson *et al.* 2000, 2004) and *An. funestus* (Wondji *et al.* 2007a,b). Despite having an unassembled genome sequence (Nene *et al.* 2007), no similar QTL mapping study has been completed for resistance-associated genome regions in *Ae. aegypti*.

QTL mapping requires constructing families from parents with distinct phenotypes (*e.g.*, permethrin susceptible or resistant). In an intercross design, F_1 siblings are allowed to randomly mate and the resulting F_2 offspring are phenotyped and genotypes are then determined at markers covering the genome at a density of ~1 marker/5 cM. A family that is continued through random intercrossing of F_2 siblings is called an advanced intercross line (AIL). AILs allow for analysis of a larger pool of siblings thus increasing the statistical power of the QTL map and creating additional generations of recombination to allow more precise determination of QTL location. In *Ae. aegypti* a dense linkage map of RFLP, RAPD, and SSCP markers, covering the three chromosomes is available (Fulton *et al.* 2001; Black and Severson 2004).

Herein, we report on the selection of a permethrin-resistant *Ae. aegypti* strain from Isla Mujeres (IMU), Quintana Roo, México. An F_3 AIL was constructed using parents from a reference-susceptible strain originally from New Orleans (Flores *et al.* 2006) and the IMU-F_4 strain that had been subjected to two generations of selection with permethrin. A total of 439 F_3 individuals were phenotyped as knockdown resistant, knocked down/recovered, or dead following permethrin exposure. We developed 34 SNP markers and mapped the locations of 21 antixenobiotic genes onto the *Ae. aegypti* linkage map. Genome regions affecting knockdown, recovery, and survival following permethrin exposure were then mapped using composite interval (Zeng 1994) and multiple interval (Kao *et al.* 1999) QTL mapping techniques.

MATERIALS AND METHODS

Mosquito collection and bioassays: Larvae from Isla Mujeres, Quintana Roo, México (latitude 21.2345, longitude 86.7316), were collected and transported to the Medical Entomology Laboratory at the Universidad Autonoma de Nuevo Leon in Monterrey, México. An F_1 was reared, blood fed, and used to generate a large F_2 generation designated IMU-F_2. F_2 eggs were sent to and hatched at Colorado State University. The concentration of permethrin that caused 50% mortality (LC_{50}) was determined by releasing 40 3- to 4-day old adults into 250 ml Wheaton bottles with the inside walls coated with a known amount of permethrin (technical grade; Chem Services, West Chester, PA) following Brogdon and McAllister (1998b). The amounts used were 0.0, 0.7, 1.0, 2.5, 5.0, and 10.0 μg active ingredient (a.i.)/bottle. Following a 1-hr exposure, mosquitoes were transferred to cardboard containers and placed into a 28° incubator with 80% relative humidity, and a 14:10 photoperiod. After 24 hr, exposed mosquitoes were recorded as alive or dead. The cumulative number of dead mosquitoes was plotted against permethrin concentration and logistic regression on SAS 9.1 (Cary, NC) was used to estimate an LC_{50} and LC_{90}. These were 2.7 and 7.0 μg a.i./bottle, respectively. The LC_{50} for the New Orleans (NO) standard susceptible strain (Flores *et al.* 2006) was consistently ~0.2 μg a.i./bottle.

Permethrin-resistant-strain selection: A separate set of adults of the IMU-F_2 generation was exposed to 5.0 μg a.i./bottle for 1 hr. Survivors were transferred to a cage and were blood fed with mice, allowing oviposition of the first selected generation designated IMU-F_3. The IMU-F_3 was hatched and adults were again exposed to a 5.0 μg a.i./bottle; survivors were allowed to mate to produce the next progeny IMU-F_4 that were used as parents for QTL mapping. Table 1 shows the survivorship and the LC_{50} for the NO strain and for IMU-F_2–IMU-F_4 generations. Mortality in NO when exposed to a 5.0-μg a.i./bottle was consistently 100%.

Mapping family crosses: For the P_1 mapping family, we crossed IMU-F_4 and NO adults. Twenty P_1 ♀IMU-F_4 × ♂NO and 20 reciprocal P_1 ♀NO × ♂IMU-F_4 crosses were made. Larvae from each line were hatched and at the pupal stage, a female (as judged by size) from one strain was transferred to

TABLE 1

Selection of the Isla Mujeres (IMU-F_4) permethrin-resistant strain

Strain	Mortality (%)	No. survivors/no. exposed	LC_{50} permethrin (μg/bottle)
New Orleans	100	0/70	0.20
IMU-F_2	83.15	125/742	2.70
IMU-F_3	9.70	857/950	17.0
IMU-F_4	0.70	883/950	60.0

Adults of each generation were exposed to 5 μg permethrin for 1 hr. Eggs were collected from the survivors in each generation.

plastic cups in cardboard containers with a male pupa from the other strain. After adults emerged, they were allowed to mate for 3 days and the P_1 male was frozen and held at −80°. Females were blood fed three times with mice over the next 10 days and the P_1 female was then frozen and held at −80°. Egg batches were maintained at room temperature for 7 days and then hatched by submersion in water followed by feeding them on Brewer's yeast. For the F_1 intercross families, one female and one male pupae from the same P_1 family were allowed to emerge, mate, and blood feed to obtain an F_2 progeny. F_2 eggs from the five largest F_1 families were hatched and siblings were intercrossed in a single cage.

Resistance phenotyping of mapping families: A portion of the adults from each of the five families were used to estimate the $LC_{50.}$ Among the five F_3 families the LC_{50} ranged from 0.7 to 1.5 μg a.i./bottle. A family with an LC_{50} of 1.2 μg a.i./bottle was chosen for the mapping study. F_3 adults that were 3–4 days old (791 total) were exposed to 1.2 μg a.i./bottle for 1 hr and adults were classified as *knockdown resistant* (*kdr*) or knocked down. Flying *kdr* mosquitoes were mechanically aspirated from the exposure bottle, transferred to a cardboard container, and frozen and held at −80°. Knocked-down mosquitoes were transferred to a different cardboard container and were maintained in an incubator at the conditions described above. Four hours later, the container was removed and flying and crawling mosquitoes were recorded as recovered and aspirated, frozen, and held at −80°. The remaining dead mosquitoes were then frozen and held at −80°. Normally mosquitoes are assayed for recovery after 24 hr, however in initial trials we obtained poor recovery of DNA from mosquitoes that had been dead for this length of time and furthermore we have routinely observed that few additional mosquitoes recover after 4 hr (our unpublished data).

DNA extraction: The DNA of the P_1 and F_1 parents, and the 439 (226 ♀ + 213 ♂) F_3 offspring was individually isolated following the DNA salt extraction method (Black and Duteau 1997) and suspended in 200 μl of TE buffer (10 mm Tris-HCl, 1 mm EDTA pH 8.0). The DNA was divided into 2- to 100-μl aliquots and stored at −80°. Many candidate genes were screened for segregation among the P_1 and F_1 adults. This required that total genomic DNA be amplified from the P_1 and F_1 DNA samples using multiple displacement amplification (Gorrochotegui-Escalante and Black 2003) with the TempliPhi 500 amplification kit (Amersham Biosciences). Amplified DNA was suspended in 90 μl ddH_2O and stored at −20°.

PCR of cDNA-SSCP markers: A total of 43 cDNA-SSCP markers (Fulton *et al.* 2001; Gomez-Machorro *et al.* 2004) and 91 CYP, EST, GST, and oxidase genes described by Strode *et al.* (2008) were tested for polymorphisms in the P_1, F_1, and ~20 F_3 mosquitoes (Tables 2 and 3). PCR products between 170 and 370 bp from CYP, EST, and GST genes were designed using Primer Premier software. PCR reaction mixture sufficient to perform 25 50-μl reactions was made by mixing 1057 μl ddH_2O, 125 μl 10 × Taq buffer (500 mm KCl, 100 mm Tris-HCL pH 9.0), 12.5 μl of 20 mm dNTPs, and 1250 pmol of each of the primers. This reaction mixture was set under a UV light source (302 nm) for 10 min, after which 10 μl of Taq DNA polymerase were added. The mixture was then dispensed into a 96-well plate. Template DNA (~100 ng) was then added to each well, followed by a drop of sterilized mineral oil. Each set of reactions was checked for contamination by the use of a negative control containing all reagents except template DNA. Samples were stored at 4° before electrophoresis. The contents of each well were tested for the presence of amplified

TABLE 2

Genetic markers with known linkage locations (Black and Severson 2004) in the *Aedes aegypti* genome and associated primers for PCR amplification

Position (cM)	Marker name	Vector base gene	Forward primer	Reverse primer	T_a	Prod. size
Chromosome I						
5	*cathbp*	AAEL007599	CAAATTCGGAACCTCACCAG	TATCCACCCTTGCATCCATC	60	343
10	*transfer*	AAEL015458	ATGCGGCCATCCAGGTTCAG	CCCGCCGACTTCAGTTTCGT	60	309
48	*ARC2*	AAEL010625	ACTACTGAGATAGGACGGAAGA	CCACTTGGACTTGGAGGT	57	260
54	*APN*	AAEL012783	TCCATCACGGCAATCACA	AGATCCAGCCAGCATTCG	57	203
Chromosome II						
28	*mucin*	AAEL004798	GACAGCACCCACAGGCAAAT	GCTCCTTTCAACGGGACCTT	60	408
43	*chymo*	AAEL014188	CCAGTTTGGCACTCGCTTCC	GACGGCAATGTCATCGGGAC	60	319
70	*sin3*	AAEL014491	GTATCTGTTCCTGCGGTTGC	CCTGAAGTGCTGCTTCTGCT	58	454
Chromosome III						
21	*malt*	AAEL009524	GGACTGGTGGGAACATGGAA	CTTATCGGACAACCGCTGGA	48	234
26	*vitgC*	AAEL003652	TGCACAGAAGACCACCAATG	TCGACTGTTCCGCTGAGTTA	60	287
32	*para*	AAEL006019	ATGTGGGATTGTATGCTTG	GATGAACCGAAATTGGAC	56	370
46	*UGALS*	AAEL010434	AGGGCTACAATCCTGGCTAT	GTATTCTGGCTGCTTGACGT	60	328
57	*apyr2*	AAEL006347	TGATTGCATCGTCGTTGATT	CAACTTGCGCTGTTTGTTTT	54	317

T_a, annealing temperature; Prod. size, product size (bp).

TABLE 3

Ninety-one selected cytochrome P450s (CYP), esterases (CCE), or glutathione transferases (GST) and various oxidase genes and associated primers and conditions for PCR amplification

Gene	Vector base	Contig	Forward primer	Reverse primer	T_a	Prod. size
			Polymorphic by SSCP			
Esterases						
CCEae1o[a]	AAEL004341	1.115	AGGTCCAGAAGCCAAACAGG	GGAAGCAGGTGTAGGTTCAGAGTA	61	394
CCEae1A	AAEL005113	1.142	CAAGAGTTGCCACTGGATGA	ATAGGCTGCCATTACGAACA	52	147
CCEae5A	AAEL005123	1.142	ACTTGGCTTTCTTTGCCTACC	CCGCTTTGAGCGATTACTTTAT	52	222
CCEjhe1F	AAEL005200	1.145	TTGTGATGAGTGGGAATGCG	TCGGTACAGTGTCAATGGGTCT	57	218
CCEunk7o[a]	AAEL008757	1.347	ACGGAGTCTTTCTTGAAGGGTAA	CACTAACTGCACGAAGCGATG	61	318
CCEunk4o	AAEL001517	1.35	CTGCTGCTGCCACATACC	CGCCGTGCTTCCAATC	57	347
CCEae2D[a]	AAEL010389	1.474	CGAGCGATTGTTATGTCTGG	AGCCCTTCTTCCGAGTTTC	57	344
CCEae4B	AAEL002376	1.55	AAACCCGAAGTGGCTTGT	GCTCTTGGTAACCGTGGC	61	359
CCEae6B	AAEL002378	1.55	CCATCGCAAAGCACCAG	TCAATAGCAAGCATTCCCTC	61	205
CCEbe2o[a]	AAEL012509	1.704	AGAAATCCGCCGAGAAAGC	GGAGTAAGGGAACCTGATGGAA	61	267
NS-COE1	AAEL003201	1.81	TATGACTAATCTTCCCATCACTCCA	GATAATGACCCGCAACCAAGT	57	212
Cytochrome P450s						
CYP304C1	AAEL014413	1.1104	CTTCCATTCGGTGCGGGTAA	TGTCGTCGTGGTTAAAGGGTTAGTT	61	277
CYP301A1	AAEL014594	1.1181	CAAGAGTGCCACAAAGCGTATGA	CAATCACGGTACTGTAAACCCTAAGAA	61	338
CYP9J24	AAEL014613	1.1188	ACTTCGCTGCTCTACACTT	TACTTGATTCCGTTTCCTT	52	211
CYP9J26	AAEL014609	1.1188	GAAACGGCGGAGCAT	GTCCACCTTGATTCCAAAA	61	370
CYP9J27v1	AAEL014616	1.1188	GATTCGCCACCGTTCA	GAGTTTCGGATACCACCAT	61	202
CYP9J28	AAEL014617	1.1188	TTTGCGAACGATGTGAT	GTTCCCGCTCCCTAAT	52	263
CYP6F2	AAEL014678	1.1219	CGAACGCAGCAAACAATGGC	CGTGTTGTAGCGGGCAAGGAT	61	305
CYP6BB2[a]	AAEL014893	1.1327	GTAGTCGCTAAGGACGGAGGAGA	GATCGTGGTGCATCGAGTGG	61	240
CYP6CD1	AAEL005006	1.138	GAAGTTGACCGTTGGATGCG	TGGTGTAATCCGTAGGCTTTCC	61	252
CYP325R1[a]	AAEL005775	1.174	GTGCTACGGTGTTCCTTGGT	CCTTTCGGTTGGGTTTCC	61	214
CYP9J10	AAEL006798	1.221	AGGGTTCGTTGAGGCA	GGTTTACCGTTCAGTGATTT	57	389
CYP9J15	AAEL006795	1.221	AAGGGCAACCTGAAGCACTCTG	TCCTCGTACAAACGGGACTGAA	61	359
CYP9J19[a]	AAEL006810	1.221	TGGACGGATAATGAGTTGA	TGTCTATGGTCGGAGGC	57	266
CYP9J8v1	AAEL006811	1.221	CTTCGCTGCCGTTATCT	TTGACACCGATTTGCTTG	57	381
CYP6AG5	AAEL006984	1.231	CTAACGAAGTCGGAGGAACG	GGGCAATGGACGAAATGA	57	287
CYP4H32[a]	AAEL007812	1.283	CGCTGCGATTACTTCCACC	TCGAACGACCGTCATCTTCA	61	282
CYP9M4	AAEL001320	1.29	CGTCGCAGCCTTCTTAGTTT	CCCAATGATAGGGTCCACCT	57	384
CYP4C52[a]	AAEL008023	1.295	TTCGACATCGTGCCCTTCAC	TTCTTGCGACAGCAACTGGTTA	61	255
CYP4G35[a]	AAEL008345	1.318	GCTTGGCGATGGGCTGTT	CATAATCAAATCCCTCCTTGCTCT	57	304
CYP6P12V2[a]	AAEL014891	1.327	GGCAGGTCACCAACAAGCA	ATCACCGATTCCCGCTCCC	57	380
CYP9J32[a]	AAEL008638	1.352	TCGGGTAATGGGACTAA	GACTCCGTTGTTTCTTGTT	52	211
CYP6AL1	AAEL008889	1.354	GCGGCTCAGGTGTTTGTG	CGGCTGTGCCTTTGTCTAT	61	350
CYP6N9	AAEL009121	1.371	GAAAGCATCCGCCAGCAT	GCAAGGTCGCCAATCCC	63	354
CYP9M8[a]	AAEL009591	1.41	ATTGAGTGGACCGATTACGACA	GGATTCGGGAAGAAATGTGG	61	358
CYP6AL3[a]	AAEL009656	1.415	ATTTGATTACTTCGCTCCGTTTGG	TGCCTGGATGTCCTGATGTCG	61	291
CYP6AG8	AAEL015654	1.4359	TGACTGTTCTCCCGAGTGTTG	GGTTTAGCGAAAGGGTGGC	61	338
CYP4AR2	AAEL010154	1.457	CACTTCGCATGTTCCCTCC	TCTTAGTGGCATTTCGTCCTG	61	208

(*continued*)

TABLE 3

(Continued)

Gene	Vector base	Contig	Forward primer	Reverse primer	T_a	Prod. size
CYP325Z1	AAEL010273	1.467	GGTGGGCAACGAAACATCTAC	AGCAGCAAACGGGACAGC	57	271
CYP12F5[a]	AAEL001960	1.47	TTTGGAAGTCACTGGCGTAAT	TTGGGCATCGGTGTTTGT	57	233
CYP305A5	AAEL002043	1.48	GGATTGTACGCTGGGAGGA	AACTTTGTATGGCTTTGGTGAGA	61	256
CYP302A1	AAEL011463	1.581	AAAAGACTGCCGTTGAGTTGG	GAGATAGGGTTGAGCCGAAGAG	61	245
CYP303A1	AAEL012144	1.66	TTGGTGAAGGCAGGAAACG	TGAATGGAAAGTGGCTGAAAA	57	282
CYP6BY1[a]		1.7	TCACGCCGCTGTTCCTATT	CCGCCACTTGTTACCTTCG	61	247
CYP6P12V1[a]	AAEL012491	1.702	GGACAGTCGGAAGCGGGAGT	GCAGCAGCAAGTTCATAAAGTCGT	61	311
CYP325M1	AAEL012773	1.738	TTGCCGACGGGCTCAA	TGGCGGGTCCTAAAGATGA	61	210
CYP4H30[a]	AAEL003399	1.85	CAATCCGCATGTTCAAGACAA	AATCGCTGACCAATACAGTTCC	61	264
CYP4J13	AAEL013555	1.869	ATGGAGTCTACAATCTGTTTGGGTAT	AACCTGCTGCGGTCGTGTC	61	319
CYP9AE1[a]	AAEL003748	1.96	CATCCTTATCGGCTTCCAGTTTT	AAGGTGGCGAGGTTTCTGCT′3	61	392
Glutathione-*S*-transferases						
GSTx1	AAEL000092	1.1	CCCAAATCAACCGAGTTCTTCA	GCCTGGTCCTCCTCGTATCCT	61	322
GSTd2	AAEL001078	1.22	TGGCGTTGAGTTGAATCCG	TGCCTCCGCAAATCGTG	61	268
GSTe2	AAEL007951	1.291	CACCCTGTCGGGCAGTGGAA	TTGGCTTGCTTAACCAGTTCTTTC	52	308
GSTe4	AAEL007962	1.291	TATTGGTTTGGACCTGGATGTT	ATAGATGATGATGGCGTGGC	57	229
GSTe5	AAEL007964	1.291	TATGGGAAGGACGATAGTTTGTA	AAGTCATCGGTCAGGGCATC	57	279
GSTe6	AAEL007946	1.291	CGATGCGGTTCTGCCGATAA	GCCAATTTCTTTGCACCTTCTC	52	208
GSTe7[a]	AAEL007948	1.291	TGTTTCCGAGACTGCG	TGACTGTTCCATCCGTTTA	52	372
GSTt3	AAEL009020	1.362	CAGAACGTGAACCGCTTTGGG	ACCTTCGCCTGATTGACTTCCA	61	260
GSTz1	Unannotated	1.632	AGCGTGCCAAGGTTCGGGAGA	GGATGATCGGATACGGGCGTAGAT	61	276
			Monomorphic by SSCP			
Esterases						
CCEunk5o	AAEL000546	1.1	CACGGAGATGATCTGGGCTAC	GCTTCAAGACGGGAACACCTAT	57	308
AaeCOE-15	AAEL004022	1.105	GATGACGGGCGTGGATTG	GGCTGTTACTATGGCAGGAAGAT	61	372
CCEae4A	AAEL005101	1.142	CGAACTGACTCGGCTACTTTC	TGCTGCCCTTCTTTACGG	50	248
CCEglt3H	AAEL000905	1.18	TGGTGCTGTCGCTGTTTCTG	CGTAAGGGTATCCACGGCTAAT	61	275
CCEae3B	AAEL002385	1.55	GCAACCCTCCAAGCCTTAA	CACCATTGTCCTTCCTACGC	57	359
Cytochrome P450s						
CYP325AA1	AAEL004012	1.105	AACGATGCGGCTCTACCCA	GAACTTCAAATCCTTTCGAGTCAAT	57	346
CYP6CB2	AAEL002872	1.1337	ATTGCCCATTCGTGCTCTG	TCTCCTCCGTGTTCCCTTTT	57	282
CYP6AK1	AAEL004941	1.136	TCTCGAAAGACAATGCAGACAAC	TCCAAATCGGCGTACAATCC	61	229
CYP325X1	AAEL005695	1.17	TGATACCGAGGAGGAATACAATAAAC	GGGCCACATAAGGCACAACC	61	335
CYP325Q1	AAEL006044	1.187	GAATGATGAAACCGATGACG	GCACTCCTCCGCAAAGC	61	386
CYP307B1v2	AAEL006875	1.224	CTCAACAACTACGACCTCAGCAT	GAGCCCACCGGAACGAA	61	248
CYP4H29	AAEL007830	1.285	TTCATCCATCCGTTCCAATCA	TCTATCGTGGCACAATCTTCACA	61	393
CYP49A1	AAEL008638	1.338	CAGAACCCAGACAAGCAGGAA	CCGTAACCGAAGGGCAAACTA	61	2000
CYP307A1	AAEL009762	1.427	GGCGAAGACGAACCAGAGCG	GGCGATGAGGAGTACCGAAGGA	61	308
CYP9M9	AAEL001807	1.43	CGGCACCAAGGTAACGG	CATCGGCACATCGGTCTTT	61	280
CYP12F6	AAEL002005	1.47	ATGATTCTGGCAGGTGTC	GGTTTCCTACTATGGGTGG	52	220

(*continued*)

products by loading 5 μl from each well onto a 1.5% (w/v) agarose gel made with Tris-Borate-EDTA buffer. DNA fragments were size fractionated by electrophoresis for 15–20 min at 112 V. Fragments were visualized by staining with Syber Green and viewing the gel over a UV transilluminator.

SSCP analysis and silver staining procedures followed Black and Duteau (1997). Polymorphic SSCP markers were sequenced in the four P_1 and F_1 parents to test for SNPs and to determine the inheritance patterns of SNP alleles. Sequences were aligned using CLUSTALW (Thompson *et al.* 1994). Allele-specific primers were designed at those loci in which genotypes were fully or partially informative in the P_1 and F_1 parents. Design of primers for melting curve PCR is fully explained in Saavedra-Rodriguez *et al.* (2007). Allele-specific fragments were detected by melting curve PCR in an Opticon 2 DNA Engine (MJ Research, Waltham MA).

Linkage mapping: Genotypes at each putative locus were entered into JoinMap 2.0 for a "recombinant inbreed RI3" cross (Stam 1993). These were tested for conformity to Mendelian ratios with a χ^2 goodness-of-fit analysis using the JMSLA procedure in JoinMap. Loci at which Mendelian genotype ratios were observed were separated into individual linkage groups using the JMGRP by increasing the minimal LOD threshold from 0.0 up to 8.0 in increments of 0.1. After markers were assigned to linkage groups, the data set was split into three groups using JMSPL. Pairwise distances (Kosambi 1943) were then estimated among loci on each of the three linkage groups using JMREC and a maximum likelihood map was estimated using JMMAP.

QTL analysis: Associations between genotypes at each marker locus and susceptibility phenotypes were initially assessed by a Fisher's exact test. The null hypothesis was that the numbers of *kdr*, recovered, and dead mosquitoes were equal in each genotype class. When the probability of the Fisher's exact test was <0.05, we examined the inheritance of the alleles at that locus. Our *a priori* hypothesis was that an excess of F_3 individuals with an allele inherited from the IMU-F_4 P_1 parent would be *kdr* or recovered following permethrin exposure while an excess of F_3 individuals with an allele inherited from the NO P_1 parent would die following exposure.

Composite interval mapping (CIM) (Zeng 1994) was then performed using QTL Cartographer 2.5 (Wang *et al.* 2007). The number of separate regions (n_p) was set to the number of regions identified in the initial Fisher's exact test and walking speed (*ws*) was set to 2 cM. Permutations ($n = 300$) were run to establish a 95% experimentwise threshold. Three separate CIM were done. First, mosquitoes with *kdr* were scored as 2, recovered as 1, and dead as 0. Next, F_3 mosquitoes with *kdr* were scored as 1, and recovered or dead were scored as 0 to test for *kdr* QTL. Lastly, surviving F_3 mosquitoes (*kdr* + recovered) were scored as 1, and dead were scored as 0 to test for survival QTL.

Multiple interval mapping (MIM) (Kao *et al.* 1999) was also performed three separate times for *kdr*, recovered, or survival phenotypes using QTL Cartographer 2.5. In each case we (1) entered QTL map positions as detected by CIM, (2) estimated QTL effects, and (3) obtained and recorded a summary. The derived model was further refined in MIM by (1) searching for new QTL, (2) estimating QTL effects, (3) obtaining and recording a summary, (4) optimizing QTL position, (5) searching for new QTL interactions, (6) testing for existing QTL main effects, (7) testing for existing QTL interaction effects, and (8) obtaining and recording a final summary.

RESULTS

Susceptibility phenotype: Of the 771 F_3 mosquitoes assayed for permethrin susceptibility, 16% (127) ex-

TABLE 3

(Continued)

Gene	Vector base	Contig	Forward primer	Reverse primer	T_a	Prod. size
CYP314A1	AAEL010946	1.524	TCCGATACAATCACCAACAATG	AATGGAAGCACCAAAGACGA	57	305
CYP325S1	AAEL000326	1.6	TGAATTTCTACGGAATATGGAAGG	AACGGACGACTGCTGTTGG	57	279
CYP315A1	AAEL011850	1.622	TTTGAAAGGATAGTGCCAGAA	GGAGCAATAGGGAACAGACG	57	323
CYP6AA5	AAEL012492	1.702	GCCCGTCATTCGCACAGT	TTCAACATCCAGCCAAAGTCC	61	210
CYP4H33	AAEL013798	1.923	CCTGATTCGCACTACCTGTG	AACTCATCCTTTCCTGCCTTA	61	395
CYP4J17	AAEL014019	1.985	CCAGGAGGAATGCGACAAACT	ACCTAACAGGCGGTAGGGAAAT	57	250
Glutathione-Stransferases						
GSTt4	AAEL004229	1.111	CCAACGGCGTCACCATTCTC	GCTGATTCAGGTTCTGCTCCATCT	61	246
GSTe1	AAEL007954	1.291	TTTCCTTTCCCTAAGTTCCGTCTC	CAGCACAAACCCATCATCGTC	49	179
GSTe3	AAEL007947	1.291	CTGGTACAGAAATACGGCAAAGA	GAACAGGGCATTCAGAGTGGA	57	297
GSTx2	AAEL010500	1.481	CGAGGCATCATCAACCAACGG	TCGGCAGATCACTCAGGTCAACA	63	268
GSTi1	AAEL011752	1.608	GCCGCTTGGGAAGTAAGTTTTG	TGATGGGATGAATTGGGTGCT	61	255

T_a, annealing temperature; Prod. size, product size (bp).
[a]Genes that were placed on the linkage map in this study.

TABLE 4

Oligonucleotides used for allele specific PCR

Gene	PCR allele-specific primers	SNP position	cM
	Chromosome I		
cathbp	[long tail]-GTGATCCGTAACCAGCGA [short tail]-GTGATCCGTAACCAGTGT ATCGGTCATGGCYGAAGC	330	5
CYP4C52	[long tail]-TGTAGAGTTTGAACATCMCGTG [short tail]-TGTAGAGTTTGAACATCMCATT GCCGATCCTGGAACAAGA	31,580	26
CYP4G35	[long tail]-AAGTTACGGTGGATATTCGGC [short tail]-AAGTTACGGTGGATATTCAGT CTCTCGCTCGTCCTCTGC	592	28
CYP6P12V2	[long tail]-CTTCGGGTTGTTATAGCTC [short tail]-CCTTCGGGTTGTTATAGTTT ACGATTCTGGTGCGGGATTTTGC	375	32
CYP6P12V1	[long tail]-AGCATCCGTAATCTTAACCCCCCAC [short tail]-AGCATCCGTAATCTTAACCCCCTAT GTTCATCTTTGCGTCGTTG	762	36
CYP9AE1	[long tail]-ATTGGTTAGCGAAACGATGCTGCAA [short tail]-ATTGGTTAGCGAAACGATGCTGTAC AGTAACTGAATCAAATCTGG	777	42
ARC2	[long tail]-CTTCTCTGGYTCATCTCCTAACATC [short tail]-CTTCTCTGGYTCATCTCCTAACGTG CGTCTGAACAAAACCCCC	−13,718	48
APN	[long tail]-GCTGATTGATGACTCGATG [short tail]-GCTGATTGATGACTCGTTC GAATGAGTTTTAGAGTGATGTCGT	2,062	54
CYP6AL3	[long tail]-GGTAYGGAAGACGATAGAAGAT [short tail]-GGTAYGGAAGACGATAGAAAAC GAAGTAATAGCTGCATCATATCYTT	762	59
CYP6BB2	[long tail]-AGTTGAAATACGATACTGTG [short tail]-AGTTGAAATACGATACTATA TGARTGCCGATTTGATGG	1,085	66
	Chromosome II		
CCEbe2o	[long tail]-ACGGATGATTAGCCAGGTAT [short tail]-ACGGATGATTAGCCAGGCAA TACAAYCCATTCTCACCGC	936	25
mucin	[long tail]-GTTGAAGAGGGAGGAGCAATA [short tail]-GTTGAAGAGGGAGGAGCAGTG CACCACAACGGCACCAGC	621	28
CYP12F5	[long tail]-GATTGTWAAGGTTGGTTTTCTTCAA [short tail]-GATTGTWAAGGTTGGTTTTCTTTAT GCTGGAATGATCTRAAGTT	624	31
CCEae2D	[long tail]-TTCACRTTTTCCGTTCGTCAA [short tail]-TTCACRTTTTCCGTTCGTTAG AAAGCCACCCCAGAAGATA	10,862	33
GSTe7	[long tail]-ACACGATACCGACCATGGA [short tail]-ACACGATACCGACCATAGT TACTTGGACACCAGATAG	231	37
chymo	[long tail]-GTCGTTTGGTTGCGGARTTCAGCG [short tail]-GTCGTTTGGTTGCGGARTTCAACA CGGGACTGACTCCYCCTTGATAG	387	43
CYP9M8	[long tail]-CGATTACGACATAGCTGCCACAGA [short tail]-CGATTACGACATAGCTGCCACGGC CATAAATAGTAAAGCAAAGTAGCG	9,874	49
CYP9J32	[long tail]-ACTGCTTCCTTGATGATTGTG [short tail]-ACTGCTTCCTTGATGATTATT AAGTTTGATGATTAAGATGGG	847	52

(*continued*)

TABLE 4

(Continued)

Gene	PCR allele-specific primers	SNP position	cM
	Chromosome III		
CYP6BY1	[long tail]-GTTCCTAAAACCCCACTTCCCGGAC [short tail]-GTTCCTAAAACCCCACTTCCCGAAT CGGTTCTTCATCTCCTCGTAG		0
CYP9J19	[long tail]-GCGACTCCTCTCAGRGACAC [short tail]-GCGACTCCTCTCAGRGATAT ACCACCATATCCAGATACTT	1,201	4
CCEae1o	[long tail]-ATCGTCTTACGCATTTTGA [short tail]-ATCGTCTTACGCATTTCGT TAGCAGAGGTGCCCGAATC	1,507	7
CCEunk7o	[long tail]-GCAAGGTTTGAATTATGTAAGTCTA [short tail]-GCAAGGTTTGAATTATGTAAGTTTT GTCGGCAAATAACTGAAA	1,236	24
CYP4H32	[long tail]-GCTGAACGGAATGTAATCGTAYCGG [short tail]-GCTGAACGGAATGTAATCGTAYTGA CTATCCAGATCCAGAACG	1,299	27
para	[long tail]-ACAAATTGTTTCCCACCCGCACCGG [short tail]-ACAAATTGTTTCCCACCCGCACTGA TGATGAACCSGAATTGGACAAAAGC	96,984	31
malt	[long tail]-ACCGTCCARATCCCCGATAGCG [short tail]-ACCGTCCARATCCCCGATAACA GAAAYTTCTACCAAGTTTACCCAA	123	33
vitgC	[long tail]-TGCCAAATGTAGCAAACG [short tail]-TGCCAAATGTAGCAAGCA TCCGCCATCACTTCTTCAGC	−86	38
CYP4H30	[long tail]-GGAGCGATTTTCCCAC [short tail]-GGAGCGATTTTCCTAA CGCTGACCAATACAGTTCCTC	19,412	41
UGALS	[long tail]-TGGATGCCGAACTACCAG [short tail]-TGGATGCCGAACTACTAA GAGCGGTCATGGTCTTGGA	433	46
CYP9J29	[long tail]-ATCGGGTCACGGTTTCCG [short tail]-ATCGGGTCACGGTTTTCA GAACGAAAATCTACGCAGCAT	1,521	50
CYP325R1	[long tail]-TGATTCTTTGGTTAATTTTCACTTA [short tail]-TGATTCTTTGGTTAATTTTCACCTT ATGGGTTGTTCTCGGCA	378	53
apyr2	[long tail]-ATTTCCAGTTTGAATCTGA [short tail]-ATTTCCAGTTTGAATCAGT GCTTTTAAGTCTCGTTTTCG	−260	68

The sequence of the long tail is 5′-GCGGGCAGGGCGGCGGGGGCGGGGCC-3′ while sequence of the short tail is 5′-GCGGGC-3′. Also listed are the map locations for each gene.

hibited *kdr* and were flying after 1-hr exposure to 1.2 μg a.i./bottle. The remainder were knocked down and immobile on the bottom of the bottle but 293 (35%) of these recovered and were flying 4 hr postexposure. These were collected and scored as recovered. The remaining 351 were scored as *dead*. Of these, 439 mosquitoes were used in QTL mapping. This included 226 females (75 *kdr*, 76 recovered, and 75 dead) and 213 males (68 *kdr*, 70 recovered, and 75 dead). The remainder of mosquitoes are stored in the freezer but were not used to reduce costs.

Marker generation: Of the 55 previously mapped cDNA-SSCP markers, 29 were polymorphic by SSCP and 12 of these were used for mapping (Table 2). Of the 235 CYP, EST, or GST genes described in Strode *et al.* (2008) we biased our selection to include those genes that were overexpressed in a microarray analysis in the Isla Mujeres strain (Strode *et al.* 2008). Of the 91 selected CYP, EST, GST, and various oxidase genes selected, 61 were polymorphic by SSCP (Table 3). Sequences of 70 of the 88 variable markers and putative resistance genes were then analyzed for informative SNPs in the P_1 and F_1 parents. On the basis of this information, 32 allele-specific PCR systems were developed to detect one SNP per gene (22 putative resistance markers and 10 genomic markers) (Table 4). *Transfer* and *sin3* were genotyped by SSCP. Sequences of the allele-specific and reverse primers, the SNP position with respect to Vectorbase (http://aaegypti.vectorbase.org/index.php) annotation,

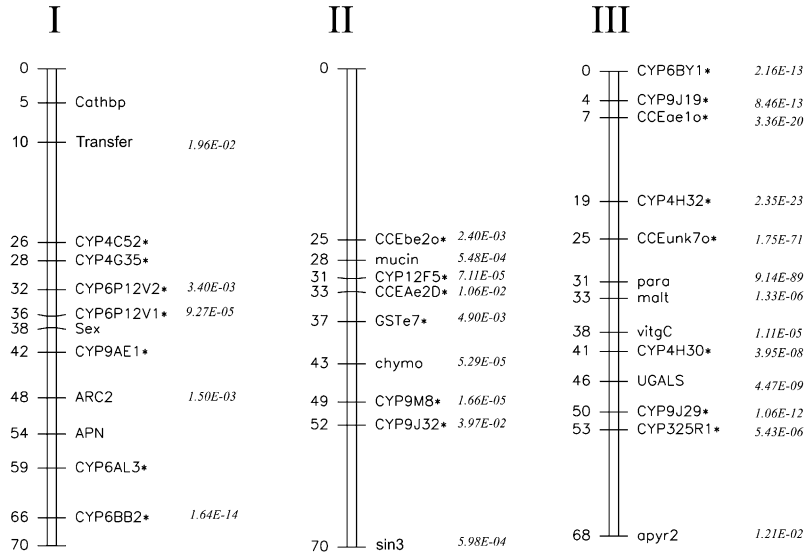

FIGURE 1.—Linkage map of cytochrome P450s (CYP), esterases (EST), or glutathione transferases (GST) in the *Aedes aegypti IMU-F_4* × *New Orleans* advanced intercross family. Linkage positions of novel insecticide resistance marker loci appear with asterisks (*). Linkage positions of the other markers are published (BLACK and SEVERSON 2004). Probabilities that the numbers of *kdr*, recovered, or dead mosquitoes were equal in each genotype class in a Fisher's exact test appear next to each locus when $P < 0.05$.

and the linkage position of the locus on the three chromosomes are shown in Table 4. Males were scored as heterozygous at the *Sex* locus while females were scored as homozygous (GILCHRIST and HALDANE 1947). The putative resistance markers included 16 CYP and 4 EST genes and 1 GST gene and the *para* gene (voltage-dependent sodium channel). The linkage location of *para* was previously mapped (SEVERSON *et al.* 1997). The *para* SNP marker identifies the *Val*1016*Iso* substitution that we had previously shown to be associated with permethrin resistance in field populations of *Ae. aegypti* (SAAVEDRA-RODRIGUEZ *et al.* 2007).

Linkage mapping: Genotypes at the 34 marker loci were analyzed in the P_1 and F_1 parents and in the 439 F_3 offspring. The probability in the Fisher's exact test appears next to markers that had a test probability <0.05 (Figure 1). The linkage positions obtained with SNP markers were mostly consistent with those published by BLACK and SEVERSON (2004). Three linkage groups were obtained with the JMGRP program in JoinMap 2.0 from an LOD threshold of 3.1–5.9. We used previously published centimorgan estimates from BLACK and SEVERSON (2004) to fix gene order on chromosomes. Figure 1 shows the linkage positions of genomic and putative resistance markers.

QTL analysis: Linkage positions derived above were entered into QTL Cartographer 2.5 along with the phenotype scores of all individuals. Scoring mosquitoes as *kdr*, recovered, or dead, CIM detected two QTL on chromosome I at map positions 38 cM and 60–65 cM and a QTL at 30 cM on chromosome II (Figure 2). At least two QTL of large effect were detected on chromosome III at map positions 24 and 31 cM. Note that the LOD scale for chromosome III in Figure 2 is ~10 times greater than those for chromosomes I and II.

Next, F_3 mosquitoes with or without *kdr* were analyzed with CIM. CIM detected the 38-cM QTL again on chromosome I and a second smaller QTL at 36 cM (Figure 2). No QTL was detected on chromosome II and 3 QTL at 10, 24, and 31 cM were detected on chromosome III. Lastly, CIM identified QTL between surviving and dead F_3 mosquitoes and detected the same 60–65 cM QTL detected earlier on chromosome I (Figure 2). A new QTL was detected on chromosome II at map position 49 cM. The two QTL of large effect were again detected on chromosome III at map positions 24 and 31 cM.

The QTL detected by CIM were entered into a MIM model to estimate the phenotypic variance (σ_p^2) for the entire model and the broad sense genotypic variance (σ_g^2) for the model and for individual QTL. MIM also calculated residual or environmental variance (σ_e^2), the map position in centimorgans, the nearest marker, and additive and dominance effects for the entire model and for individual QTL (Table 5). Models were developed for the three phenotype comparisons (*kdr*, recovered, and dead), for *kdr*, and for survival. The σ_p^2 was largest (0.6672) for the three phenotype comparisons and σ_g^2 accounted for 70% of this variance. Most (59.3%) of σ_p^2 was accounted for by chromosome III QTL at map positions 24.6 (16.4%) and 31 cM (42.9%). The nearest markers to these were *CCEunk7o* and *para*, respectively.

The MIM model for *kdr* had the largest percentage (84.1%) of σ_p^2 accounted for by σ_g^2. Again, most (79.1%) of σ_p^2 is accounted for by chromosome III QTL at map positions 24.7 (20.5%) and 31 cM (58.6%). The MIM model for survival had the smallest percentage (36.8%) of σ_p^2 accounted for by σ_g^2. The chromosome III QTL at map positions 24.7 (9.3%) and 31 cM (23.1%) accounted for most of σ_g^2.

Individual QTL effects on each phenotype: Clearly the chromosome III QTL at 24.7 and 31 cM had the largest effects on knockdown, recovery, and survival. The closest markers to these QTL were *CCEunk7o* at 24 cM and the *Val*1016*Iso* substitution in *para* at 31 cM. The

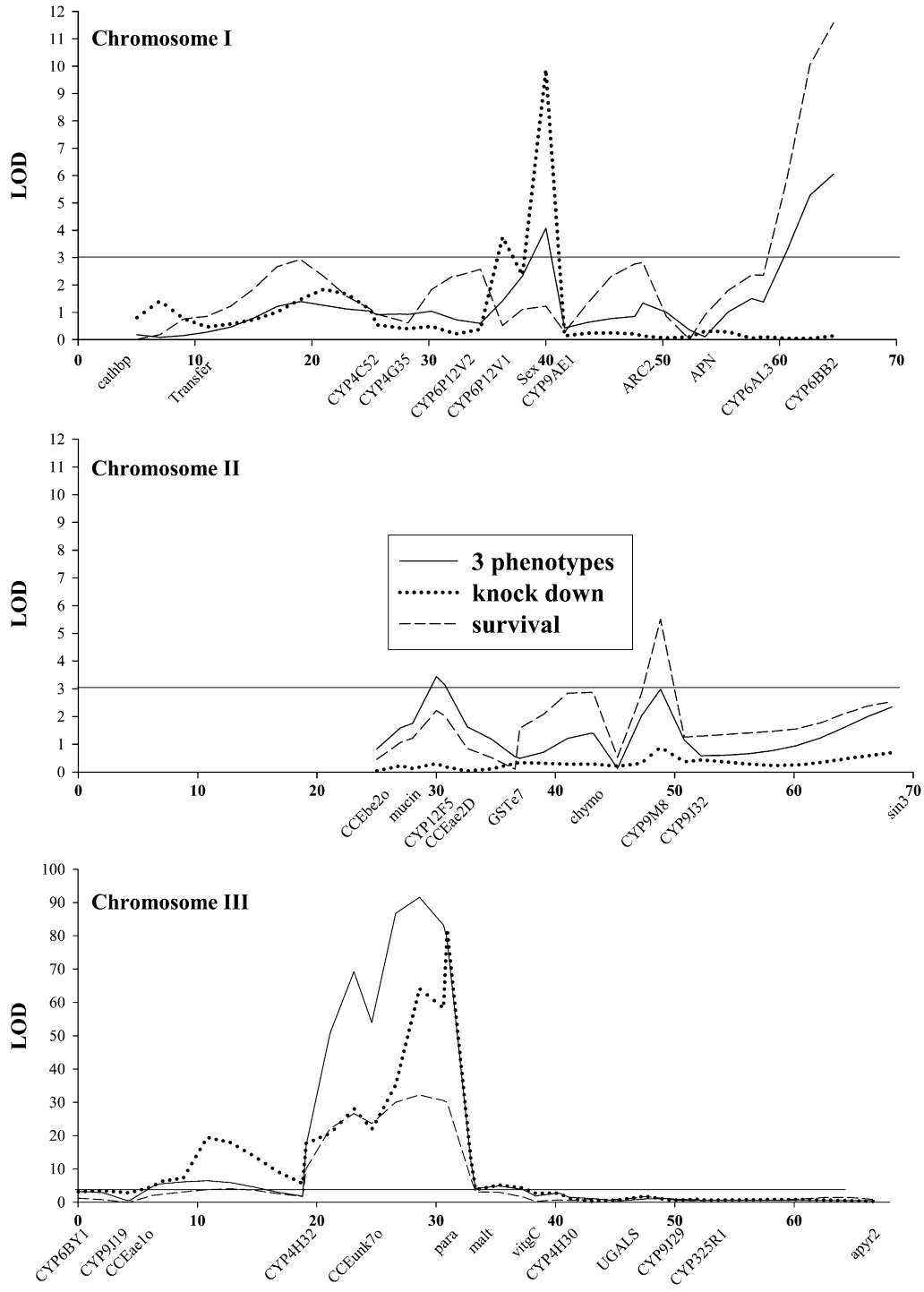

FIGURE 2.—Plot of LOD values associated with *kdr*, recovery, or survival along chromosomes I–III in the *Aedes aegypti IMU-F*$_4$ × *New Orleans* advanced intercross family. LOD values were estimated by composite interval mapping in QTL Cartographer 2.5 (WANG *et al.* 2007). Names of markers are listed along the *x*-axis to orient QTL positions relative to Figure 1.

knockdown, recovery, and survival rates for each of the three *para* and *CCEunk7o* genotypes are shown for females and males separately in Figure 3. At both QTL susceptibility alleles inherited from the New Orleans susceptible (S) parent were dominant in their effects on knockdown. Heterozygotes and S homozygotes had a 0.8–1.0 knockdown rate while homozygotes for alleles inherited from the Isla Mujeres resistant (R) parent had a 0.0–0.1 knockdown rate (Figure 3A). In contrast, genotypes at both QTL appeared to be overdominant on their effects on recovery (Figure 3B). Recovery was 0.5–0.6 in heterozygotes but 0.0–0.3 in either of the homozygote classes. However, note that the 95% confidence intervals surrounding R/R estimates were large because very few mosquitoes with this genotype were actually knocked down. A third pattern of QTL effects was seen with survival (Figure 3C). Among R homozygotes, the survival rate was 0.9–1.0, 0.6–0.7 among heterozygotes, and 0.0–0.4 for S homozygotes. Differences among females and males were not significant.

TABLE 5

Multiple-interval mapping estimates of QTL position and associated genetic, environmental, and phenotypic variance and additive and dominance effects associated with knockdown, recovery and survival QTL in *Aedes aegypti*

σ^2_g	σ^2_P (%)	σ^2_e	σ^2_P (%)	σ^2_P	Nearest marker	cM	Additive/dominance	Effect	σ^2_P (%)
					Knockdown, recovery, and dead				
0.4671	70	0.2001	30	0.6672	*SEX*	38.1	A	0.0642	0.1
						(38–41.6)	D	−0.0942	0.2
					CYP6BB21	65.0	A	0.0967	1.2
						(58.6–65.9)	D	0.1905	2.7
					CYP12F5	30.9	A	0.1163	1.4
						(30.8–32.7)	D	0.0855	0.4
					CCEae1o	6.9	A	0.3585	9.2
						(6.8–18.9)	D	0.2693	−5.8
					CYP4H32	19.1	A	0.0399	1.4
						(19–24.5)	D	0.0407	−0.2
					CCEunk7o	24.6	A	0.2785	15.5
						(24.5–30.8)	D	−0.0486	0.9
					Para	31.0	A	0.6138	35.7
						(30.9–33.3)	D	−0.3082	7.2
					Knockdown				
0.1846	84.1	0.0350	15.9	0.2196	*CYP6P12v1*	36.4	A	−0.0514	0.1
						(36.3–38)	D	−0.0014	0.0
					Sex	38.1	A	0.0557	0.1
						(38–41.6)	D	−0.0111	0.0
					CYP9J19	4.4	A	−0.4795	−18.4
						(4.3–20.8)	D	−0.4523	17.1
					CCEae1o	6.9	A	0.6019	28.2
						(6.8–10)	D	0.5261	−22.5
					CYP4H32	19.2	A	0.0112	0.6
						(19.1–21.5)	D	0.0189	−0.4
					CCEunk7o	24.7	A	0.1378	13.8
						(24.6–27.8)	D	−0.1190	6.7
					Para	31	A	0.3561	37.1
						(30.9–33.3)	D	−0.3360	21.5
					Survival				
0.0828	36.8	0.1422	63.2	0.2249	*CYP6BB21*	65.0	A	0.0248	0.2
						(58.6–65.9)	D	0.0743	0.8
					CYP9M8	48.9	A	−0.1851	3.1
						(48.8–52.2)	D	−0.0411	0.1
					CCEunk7o	24.7	A	0.1376	9.3
						(24.6–28.4)	D	0.1238	0.0
					Para	31	A	0.3175	22.9
						(30.9–33.3)	D	−0.0230	0.2

Two additional QTL on chromosome III were also detected and the closest associated markers were *CCEae1o* at 7 cM and *CYP4H32* at 19 cM (Figure 2). At the 7-cM QTL, the effect of the S allele on knockdown was partially dominant (Figure 4A) with half of R homozygotes knocked down, 0.85–0.95 of heterozygotes knocked down and all S homozygotes knocked down. At the 19-cM QTL, the S allele was also partially dominant in affecting knockdown (Figure 4A) with 0.25 of R homozygotes knocked down, 0.7–0.8 of heterozygotes knocked down, and 0.80–0.85 of S homozygotes knocked down. At the 7-cM QTL, the R allele appears to be dominant to the S allele in conditioning recovery (Figure 4B) with half of R homozygotes and heterozygotes recovering but none of the S homozygotes recovering. Alleles at the 19-cM QTL appeared to be additive in conditioning the recovery rate in males with 0.80 recovery in R homozygotes, 0.55 in heterozygotes, and 0.15 in S homozygotes (Figure 4B). In contrast, recovery appeared to follow a pattern of overdominance in females at this QTL, with 0.4 of females homozygous for either alleles recovering but 0.6 of heterozygous females recovering. The R allele at the 7-cM QTL was also partially dominant in its effect on survival (Figure 4C) with 0.75 of R homozygotes surviving, 0.60 of heterozygotes surviving, and no S homozygotes surviving. Alleles at the 19-cM QTL appeared to be additive in conditioning survival and there were sex-specific differences. Male R homozygotes had 0.95 survival while

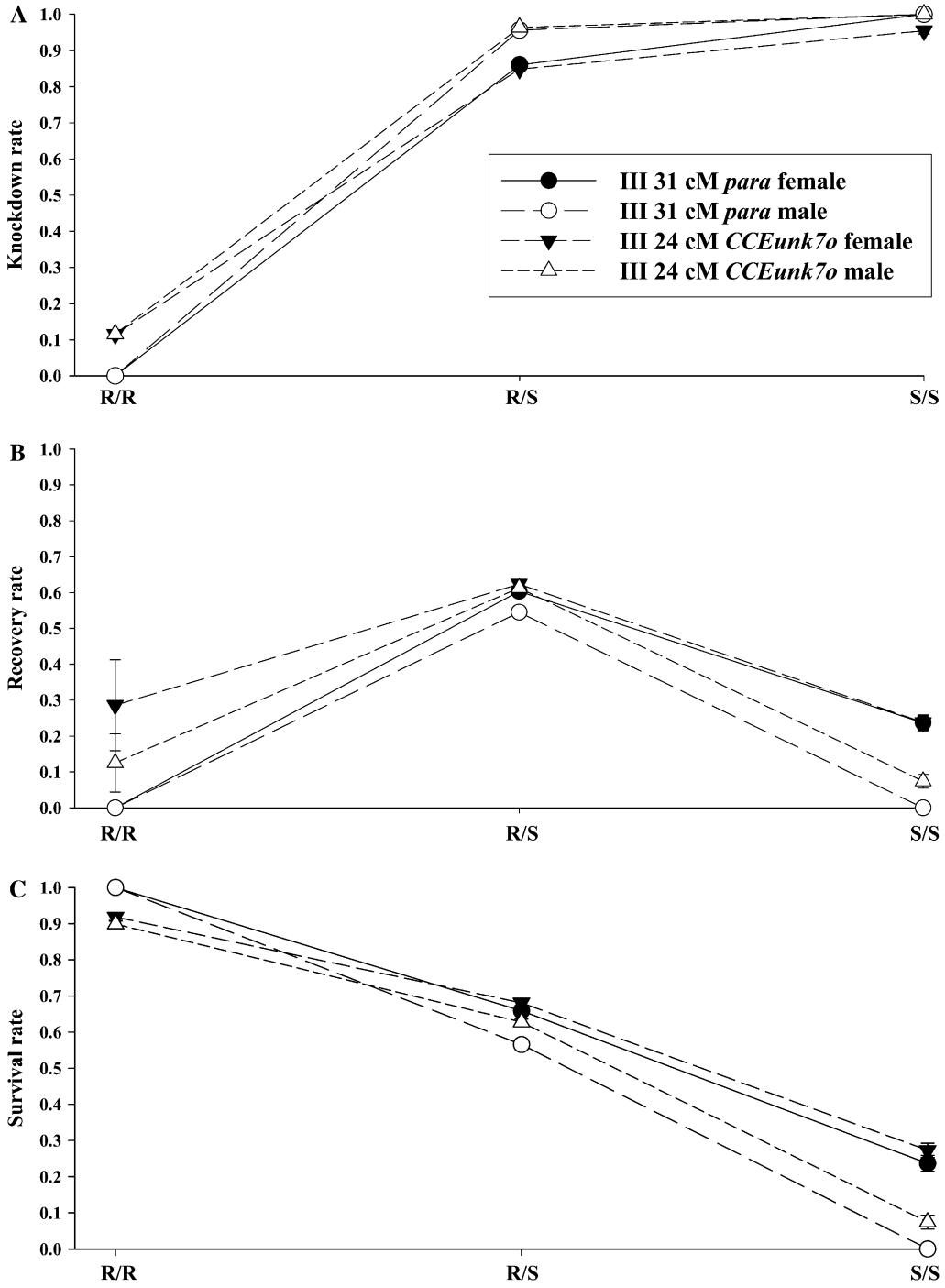

FIGURE 3.—Plot of knockdown, recovery, and survival rates as a function of F_3 genotypes at the *para* and *CCEunk7o* loci. R/R indicates that both alleles were inherited from the *IMU-F4* resistant P_1 parent; S/S indicates that both alleles were inherited from the *New Orleans* susceptible P_1 parent; R/S indicates heterozygotes. (A) Knockdown rate [1 − (no. *kdr*/ no. total)] as a function of F_3 genotypes. (B) Recovery rate [no. recovered /(no. recovered + no. dead)] as a function of F_3 genotypes. (C) Survival rate [(no. *kdr* + no. recovered)/no. total] as a function of F_3 genotypes.

0.65 of heterozygotes and 0.25 of S homozygotes survived. In contrast, female R homozygotes had 0.85 survival while 0.7 of heterozygotes and 0.45 of S homozygotes survived.

QTL of relatively minor effect were detected on chromosome I at positions 36, 38, and 66 cM and on chromosome II at 30 and 49 cM (Figure 2). The 36-cM (nearest marker, *CYP6P12V1*) and 38 cM (nearest marker, *Sex*) QTL were associated with knockdown. Because equal numbers of male and female mosquitoes from the three phenotypic classes were selected for genotyping, we could not analyze knockdown with regards to *Sex*. However, the 38-cM QTL probably reflects differences in knockdown rates between sexes (Figures 4A and 5A). The 36-cM QTL near *CYP6P12V1* is interesting in that, contrary to our *a priori* hypothesis the R homozygotes have a 0.05–0.20 greater knockdown rate than the heterozygotes or S homozygotes (Figure 5A).

The 38-cM (nearest marker, *Sex*) and 66-cM (nearest marker, *CYP6BB2*) QTL and the 31-cM QTL on chromosome II affected recovery rate (Figure 5B). Again, note that the recovery rate differed between the sexes at the QTL near *CYP4H32* (Figure 4B) and at the QTL near

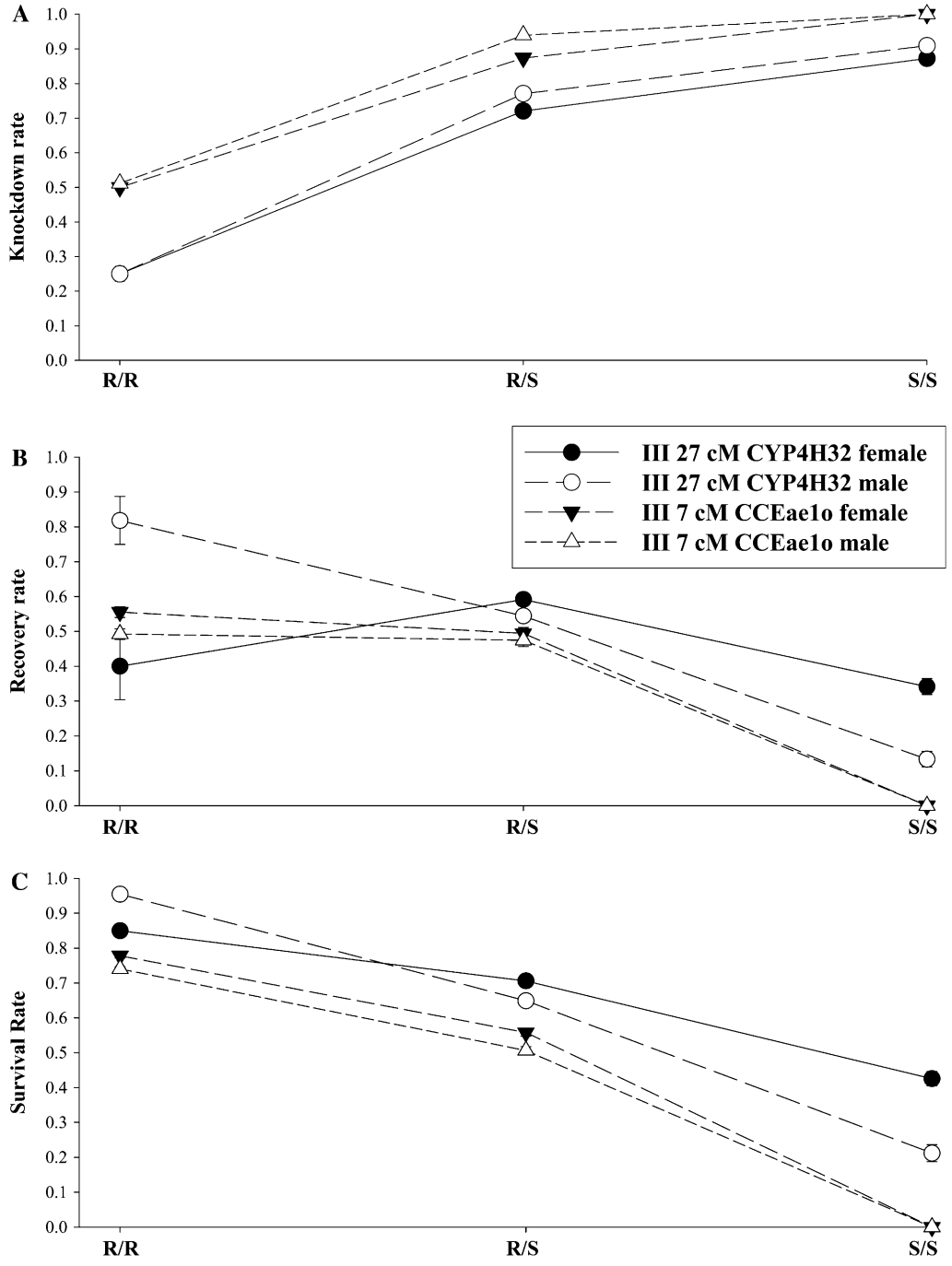

FIGURE 4.—Plot of knockdown, recovery, and survival rates as a function of F_3 genotypes at the *CCEae1o* and *CYP4H32* loci. Labels along the abscissa and rates along the ordinate axis are as explained in Figure 3.

CYP6BB2 and *CYP6P12V1* markers (Figure 5B). Genotypes at the 66-cM QTL were overdominant with a recovery rate of 0.55–0.70 among R homozygotes, 0.65–0.90 among heterozygotes, and 0.2–0.30 among S/S homozygotes (Figure 5B).

QTL affecting survival (Figure 5C) were detected on chromosome I at 66 cM and on chromosome II at 49 cM. Survival among genotypes at the QTL near *CYP6BB2* differed between sexes. Female R homozygotes had 0.75 survival while 0.55 of males survived. Among heterozygotes, 0.9 of females survived while 0.8 of males survived. Male and female S homozygotes had an equal survival rate of 0.55 (Figure 5C). Survival among genotypes at the 49-cM QTL on chromosome II followed a partially dominant pattern in females with 0.65 survival among R homozygotes and heterozygotes and 0.75 among S homozygotes (Figure 5C) but an additive pattern was noted in males with 0.45 survival among R homozygotes, 0.60 among heterozygotes, and all S homozygotes survived.

DISCUSSION

We used artificial selection to produce in just two generations a strain of *Ae. aegypti* with ~24-fold greater

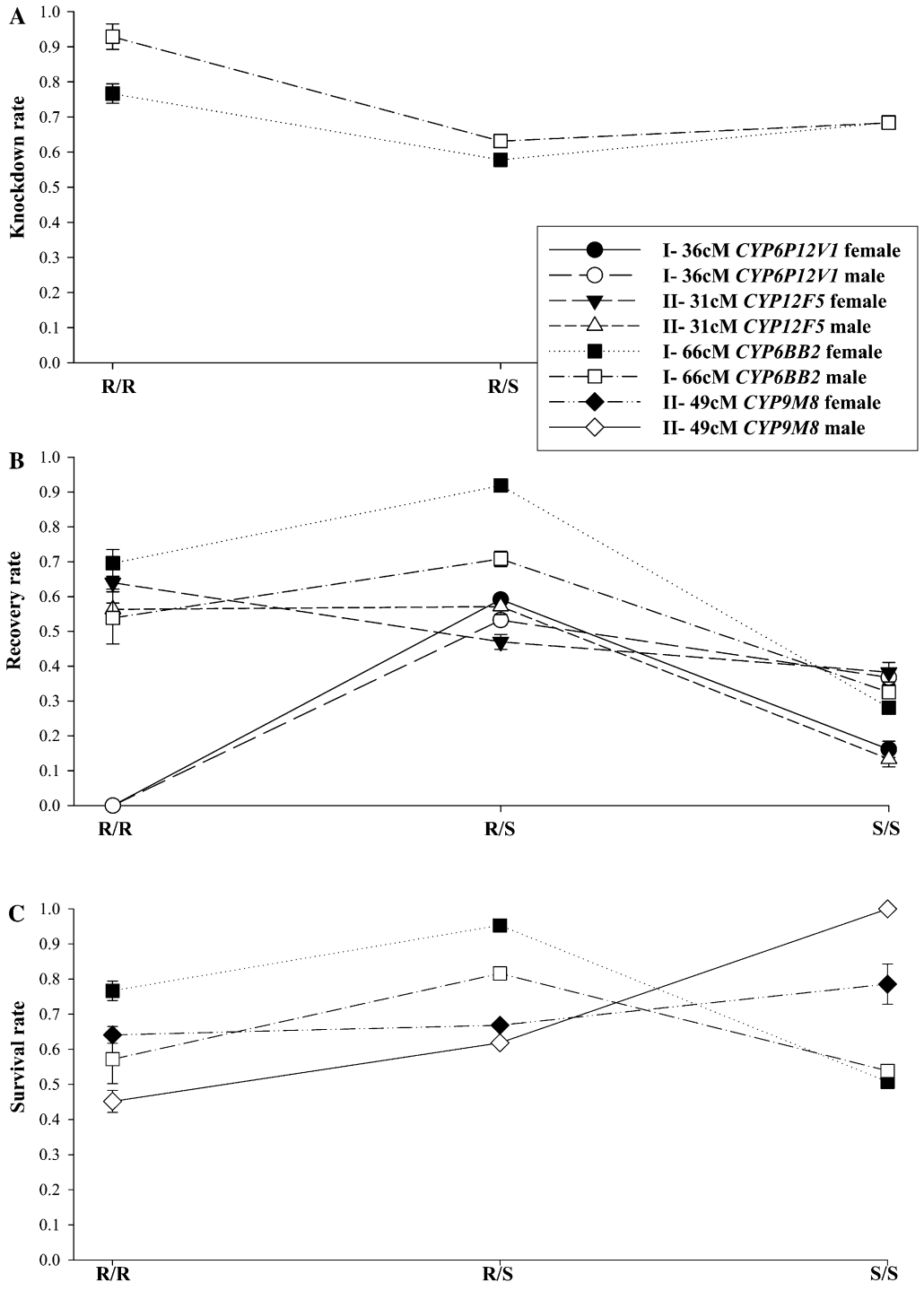

FIGURE 5.—Plot of knockdown, recovery, and survival rates as a function of F_3 genotypes at the *CYP6BB2* and *CYP6P12V1* loci on chromosome I and *CYP12F5* and *CYP9M8* on chromosome II. Labels along the abscissa and rates along the ordinate axis are as explained in Figure 3.

resistance to permethrin than the original, unselected Isla Mujeres collection and ~300-fold greater resistance than the New Orleans standard susceptible strain (Table 1). In this selected strain, we detected five *kdr* QTL near markers *CYP6P12V1* and *Sex* on chromosome I and near markers *CCEae1o*, *CYP4H32*, *CCEunk7o*, and *para* on chromosome III. Three QTL that condition recovery were detected on chromosome I near *CYP6BB2*, on chromosome II near *CYP12F5*, and on chromosome III near *CCEunk7o* and *para*. One additional QTL conditioned survival and was located on chromosome II near *CYP9M8*.

The chromosome III 24- and 31-cM QTL accounted for 59.3% of σ_p^2 for knockdown, recovery, or death, 79.1% of knockdown σ_p^2, and 31.3% of σ_p^2 for survival. The large contributions by the 31-cM QTL to *kdr* were expected and corresponded to a previously characterized *Val* → *Iso* replacement substitution at codon 1016 in hydrophobic segment 6 of domain II of *para*. We found this mutation to be associated with *kdr* in *Ae.*

aegypti populations from throughout Latin America (Saavedra-Rodriguez *et al.* 2007). Generally mutations in this region of *para* in insects reduce permethrin binding and allow normal functioning of the sodium-gated channels in neuronal membranes (Soderlund and Knipple 2003).

What remains unclear is whether the 24-cM QTL nearest *CCEunk7o* represents an independent *kdr* QTL or is a marker that was swept along during selection for *kdr* associated with the nearby *para* locus. In the QTL analyses, genotypes at *CCEunk7o* and *para* were not independent. We had no knowledge of the *Val*1016*Iso* substitution when this mapping study was initiated and so we could not have selected out this mutation prior to performing the F_1 intercrosses.

Despite the rapid response to selection, the QTL patterns that we have detected suggest that a diversity of loci and mechanisms in the *Ae. aegypti* genome respond to selection for pyrethroid resistance. Furthermore, these loci condition different phenotypes associated with resistance evolution. Some determine whether knockdown occurs (Figures 3A–5A), while others affect recovery following knockdown (Figures 3B–5B) and at least one QTL (Figure 5C) exclusively affected survival. The genes underlying these QTL probably act sequentially in determining the overall resistance response. QTL that prevent or reduce pyrethroid binding in the sodium-gated channels prevent knockdown. However, among knocked-down mosquitoes, other QTL may affect the subsequent metabolic degradation of the pesticide, ultimately removing pyrethroid from their systems and allowing these mosquitoes to recover. None of the three MIM models displayed in Table 5 accounted for all of the σ_P^2. From 15.9 to 56.5% of σ_P^2 was residual variance, cumulatively unaccounted for by the identified QTL. Thus "environmental," uncontrolled factors in experimental design and execution also account for a substantial part of σ_P^2 in resistance. Our QTL map contains 34 markers that cover 174 cM of the 204-cM *Ae. aegypti* linkage map (Black and Severson 2004). There was a 16-cM gap in marker coverage on the top of chromosome I, a 25-cM and 18-cM gap at the top and bottom of chromosome II, respectively, and a 15-cM gap at the bottom of chromosome III. The largest gap unbounded by a marker was at the top of chromosome II. Nine markers on the top of chromosome II were tested but none were informative. Thus it is possible that the top of chromosome II contained additional resistance QTL.

This study represents only two collections of *Ae. aegypti*. An obvious question is whether other geographic populations, or even replicate collections from Isla Mujeres, would respond in the same way to selection with pyrethroids. This is being addressed by exploring for other QTL using mosquitoes from different geographic locations. The polygenic, quantitative genetic patterns that we have observed in these experiments are supported by earlier studies that approached insecticide resistance evolution as a quantitative rather than discrete genetic character (Roush and McKenzie 1987; Firko and Hayes 1990; Ferrari and Georghiou 1991; Morton 1993; Roush 1993; Guillemaud *et al.* 1999; Paton *et al.* 2000; Oakeshott *et al.* 2003). Furthermore, of the few insecticide resistance QTL mapping studies completed to date, all have reported multiple regions that respond to selection with insecticides (Ranson *et al.* 2000, 2004; Hawthorne 2003; Jallow and Hoy 2006; Wondji *et al.* 2007c).

This work was supported by the Innovative Vector Control Consortium.

LITERATURE CITED

Bisset, J., M. M. Rodriguez and D. Fernandez, 2006 Selection of insensitive acetylcholinesterase as a resistance mechanism in *Aedes aegypti* (Diptera: Culicidae) from Santiago de Cuba. J. Med. Entomol. **43:** 1185–1189.

Black, W. C., and N. M. DuTeau, 1997 RAPD-PCR and SSCP analysis for insect population genetic studies, pp. 361–373 in *The Molecular Biology of Insect Disease Vectors: A Methods Manual*, edited by J. Crampton, C. B. Beard, and C. Louis. Chapman & Hall, New York.

Black, W. C., and D. W. Severson, 2004 Genetics of vector competence, pp. 415–448 in *Biology of Disease Vectors*, Ed. 2, edited by W. C. Marquardt. Elsevier, Amsterdam.

Brogdon, W. G., and J. C. McAllister, 1998a Insecticide resistance and vector control. Emerging Infect. Dis. **4:** 605–613.

Brogdon, W. G., and J. C. McAllister, 1998b Simplification of adult mosquito bioassays through use of time-mortality determinations in glass bottles. J. Am. Mosq. Control Assoc. **14:** 159–164.

David, J. P., C. Strode, J. Vontas, D. Nikou, A. Vaughan *et al.*, 2005 The *Anopheles gambiae* detoxification chip: a highly specific microarray to study metabolic-based insecticide resistance in malaria vectors. Proc. Natl. Acad. Sci. USA **102:** 4080–4084.

Ferrari, J. A., and G. P. Georghiou, 1991 Quantitative genetic variation of esterase activity associated with a gene amplification in *Culex quinquefasciatus*. Heredity **66**(Pt 2): 265–272.

Firko, M. J., and J. L. Hayes, 1990 Quantitative genetic tools for insecticide resistance risk assessment: estimating the heritability of resistance. J. Econ. Entomol. **83:** 647–654.

Flores, A. E., W. Albeldano-Vazquez, I. F. Salas, M. H. Badii, H. L. Becerra *et al.*, 2005 Elevated alpha-esterase levels associated with permethrin tolerance in *Aedes aegypti* (L.) from Baja California, Mexico. Pest. Biochem. Physiol. **82:** 66–78.

Flores, A. E., J. S. Grajales, I. F. Salas, G. P. Garica, M. H. L. Becerra *et al.*, 2006 Mechanisms of insecticide resistance in field populations of *Aedes aegypti* (L.) from Quintana Roo, Southern Mexico. J. Am. Mosq. Control Assoc. **22:** 672–677.

Fulton, R. E., M. L. Salasek, N. M. DuTeau and W. C. Black, 2001 SSCP analysis of cDNA markers provides a dense linkage map of the *Aedes aegypti* genome. Genetics **158:** 715–726.

Gilchrist, B. M., and J. B. S. Haldane, 1947 Sex linkage and sex determination in a mosquito, *Culex molestus*. Hereditas **33:** 175–190.

Gomez-Machorro, C., K. E. Bennett, M. D. Munoz and W. C. Black, 2004 Quantitative trait loci affecting dengue midgut infection barriers in an advanced intercross line of *Aedes aegypti*. Insect Mol. Biol. **13:** 637–648.

Gorrochotegui-Escalante, N., and W. C. Black, 2003 Amplifying whole insect genomes with multiple displacement amplification. Insect Mol. Biol. **12:** 195–200.

Gubler, D., 2005 The emergence of epidemic dengue fever and dengue hemorrhagic fever in the Americas: a case of failed public health policy. Rev. Panam. Salud Publica-Panamer. J. Publ Health **17:** 221–224.

Guillemaud, T., M. Raymond, A. Tsagkarakou, C. Bernard, P. Rochard *et al.*, 1999 Quantitative variation and selection of esterase gene amplification in *Culex pipiens*. Heredity **83:** 87–99.

Hawthorne, D. J., 2003 Quantitative trait locus mapping of pyrethroid resistance in Colorado potato beetle, *Leptinotarsa decemlineata* (Say) (Coleoptera: Chrysomelidae). J. Econ. Entomol. **96:** 1021–1030.

Jallow, M. F., and C. W. Hoy, 2006 Quantitative genetics of adult behavioral response and larval physiological tolerance to permethrin in diamondback moth (Lepidoptera: Plutellidae). J. Econ. Entomol. **99:** 1388–1395.

Kao, C. H., Z. B. Zeng and R. D. Teasdale, 1999 Multiple interval mapping for quantitative trait loci. Genetics **152:** 1203–1216.

Kosambi, D. D., 1943 The estimation of map distances from recombination values. Ann. Eugen. **12:** 172–175.

Morton, R. A., 1993 Evolution of *Drosophila* insecticide resistance. Genome **36:** 1–7.

Nene, V., J. R. Wortman, D. Lawson, B. Haas, C. Kodira *et al.*, 2007 Genome sequence of *Aedes aegypti*, a major arbovirus vector. Science **316:** 1718–1723.

Norma Oficial Mexicana, 2003 NOM-032-SSA-2–2002 para la vigilancia epidemiologica, prevencion y control de enfermedades transmitidas por vector (D.O.F. 21 julio del 2003). Norma Oficial Mexicana, Mexico City.

Oakeshott, J. G., I. Home, T. D. Sutherland and R. J. Russell, 2003 The genomics of insecticide resistance. Genome Biol. **4:** 202.

Paton, M. G., S. H. Karunaratne, E. Giakoumaki, N. Roberts and J. Hemingway, 2000 Quantitative analysis of gene amplification in insecticide-resistant *Culex* mosquitoes. Biochem. J. **346**(Pt 1): 17–24.

Pedra, J. H. F., R. A. Festucci-Buselli, W. L. Sun, W. M. Muir, M. E. Scharf *et al.*, 2005 Profiling of abundant proteins associated with dichlorodiphenyltrichloroethane resistance in *Drosophila melanogaster*. Proteomics **5:** 258–269.

Ranson, H., B. Jensen, X. Wang, L. Prapanthadara, J. Hemingway *et al.*, 2000 Genetic mapping of two loci affecting DDT resistance in the malaria vector *Anopheles gambiae*. Insect Mol. Biol. **9:** 499–507.

Ranson, H., M. G. Paton, B. Jensen, L. McCarroll, A. Vaughan *et al.*, 2004 Genetic mapping of genes conferring permethrin resistance in the malaria vector, *Anopheles gambiae*. Insect Mol. Biol. **13:** 379–386.

Rodriguez, M. M., J. Bisset, D. M. De Fernandez, L. Lauzan and A. Soca, 2001 Detection of insecticide resistance in *Aedes aegypti* (Diptera: Culicidae) from Cuba and Venezuela. J. Med. Entomol. **38:** 623–628.

Rodriguez, M. M., J. Bisset, M. Ruiz and A. Soca, 2002 Cross-resistance to pyrethroid and organophosphorus insecticides induced by selection with temephos in *Aedes aegypti* (Diptera: Culicidae) from Cuba. J. Med. Entomol. **39:** 882–888.

Rodriguez, M. M., J. A. Bisset, Y. De Armas and F. Ramos, 2005 Pyrethroid insecticide-resistant strain of *Aedes aegypti* from Cuba induced by deltamethrin selection. J. Am. Mosq. Control Assoc. **21:** 437–445.

Roush, R. T., 1993 Occurrence, genetics and management of insecticide resistance. Parasitol. Today **9:** 174–179.

Roush, R. T., and J. A. McKenzie, 1987 Ecological genetics of insecticide and acaricide resistance. Annu. Rev. Entomol. **32:** 361–380.

Saavedra-Rodriguez, K., L. Urdaneta-Marquez, S. Rajatileka, M. Moulton, A. E. Flores *et al.*, 2007 A mutation in the voltage-gated sodium channel gene associated with pyrethroid resistance in Latin American *Aedes aegypti*. Insect Mol. Biol. **16:** 785–798.

Severson, D. W., N. M. Anthony, O. Andreev and R. H. ffrench-Constant, 1997 Molecular mapping of insecticide resistance genes in the yellow fever mosquito (*Aedes aegypti*). J. Hered. **88:** 520–524.

Soderlund, D. M., and D. C. Knipple, 2003 The molecular biology of knockdown resistance to pyrethroid insecticides. Insect Biochem. Mol. Biol. **33:** 563–577.

Stam, P., 1993 Construction of integrated genetic-linkage maps by means of a new computer package: Joinmap. Plant J. **3:** 739–744.

Strode, C., C. S. Wondji, J. P. David, N. J. Hawkes, N. Lumjuan *et al.*, 2008 Genomic analysis of detoxification genes in the mosquito *Aedes aegypti*. Insect Biochem. Mol. Biol. **38:** 113–123.

Thompson, J. D., D. G. Higgins and T. J. Gibson, 1994 Clustal-W: improving the sensitivity of progressive multiple sequence alignment through sequence weighting, position-specific gap penalties and weight matrix choice. Nucleic Acids Res. **22:** 4673–4680.

Vontas, J., J. P. David, D. Nikou, J. Hemingway, G. K. Christophides *et al.*, 2007 Transcriptional analysis of insecticide resistance in *Anopheles stephensi* using cross-species microarray hybridization. Insect Mol. Biol. **16:** 315–324.

Wang, S., C. J. Basten and Z.-B. Zeng, 2007 Windows QTL Cartographer 2.5. North Carolina State University, Raleigh, NC.

Wondji, C. S., J. Hemingway and H. Ranson, 2007a Identification and analysis of single nucleotide polymorphisms (SNPs) in the mosquito *Anopheles funestus*, malaria vector. BMC Genomics **8:** 5.

Wondji, C. S., J. Morgan, M. Coetzee, R. H. Hunt, K. Steen *et al.*, 2007b Mapping a quantitative trait locus (QTL) conferring pyrethroid resistance in the African malaria vector Anopheles funestus. BMC Genomics **8:** 34.

Zeng, Z. B., 1994 Precision mapping of quantitative trait loci. Genetics **136:** 1457–1468.

Communicating editor: L. G. Harshman